Received: 24 November 2022 | Revised: 5 June 2023 | Accepted: 21 June 2023

DOI: 10.1002/biot.202200554

Biotechnology Journal

RESEARCH ARTICLE

Design and evaluation of a 3D-printed, lab-scale perfusion bioreactor for novel biotechnological applications

Manuel Merkel[1] | **Philipp Noll**[2] | **Lars Lilge**[1,3] | **Rudolf Hausmann**[1] | **Marius Henkel**[2]

[1]Department of Bioprocess Engineering (150k), University of Hohenheim, Stuttgart, Germany

[2]Cellular Agriculture, TUM School of Life Sciences, Technical University of Munich, Freising, Germany

[3]Department of Molecular Genetics, University of Groningen, AG, Groningen, The Netherlands

Correspondence
Marius Henkel, Cellular Agriculture, TUM School of Life Sciences, Technical University of Munich, Freising, Germany.
Email: marius.henkel@tum.de

Funding information
Ministerium für Wissenschaft, Forschung und Kunst Baden-Württemberg, Grant/Award Number: MM is a member of the "BBW ForWerts" graduate program; Bundesministerium für Bildung und Forschung, Grant/Award Number: 031B0673C

Abstract

3D-printing increased in significance for biotechnological research as new applications like lab-on-a-chip systems, cell culture devices or 3D-printed foods were uncovered. Besides mammalian cell culture, only few of those applications focus on the cultivation of microorganisms and none of these make use of the advantages of perfusion systems. One example for applying 3D-printing for bioreactor development is the microbial utilization of alternative substrates derived from lignocellulose, where dilute carbon concentrations and harmful substances present a major challenge. Furthermore, quickly manufactured and affordable 3D-printed bioreactors can accelerate early development phases through parallelization. In this work, a novel perfusion bioreactor system consisting of parts manufactured by fused filament fabrication (FFF) is presented and evaluated. Hydrophilic membranes are used for cell retention to allow the application of dilute substrates. Oxygen supply is provided by membrane diffusion via hydrophobic polytetrafluoroethylene membranes. An exemplary cultivation of *Corynebacterium glutamicum* ATCC 13032 supports the theoretical design by achieving competitive biomass concentrations of 18.4 g L^{-1} after 52 h. As a proof-of-concept for cultivation of microorganisms in perfusion mode, the described bioreactor system has application potential for bioconversion of multi-component substrate-streams in a lignocellulose-based bioeconomy, for in-situ product removal or design considerations of future applications for tissue cultures. Furthermore, this work provides a template-based toolbox with instructions for creating reference systems in different application scenarios or tailor-made bioreactor systems.

KEYWORDS
3D-printing, bioeconomy, *Corynebacterium glutamicum*, membrane bioreactor, perfusion bioreactor process

Abbreviations: ABS, acrylonitrile butadiene styrene; CAD, computer-aided design; CPE, co-polyester; DO, dissolved oxygen; FFF, fused filament fabrication; iD, inner diameter; MOPS, morpholino propanesulfonic acid; oD, outer diameter; OD_{600nm}, optical density; PTFE, polytetrafluoroethylene; PVDF, polyvinylidene difluoride; TES, trace element solution.

1 | INTRODUCTION

Additive manufacturing or 3D-printing is a novel manufacturing technique that has advanced from a tool for creation of demonstration models to real world industrial applications.[1] Its main benefits in comparison to conventional manufacturing methods are high flexibility regarding design choices and short manufacturing times.[2] There are different 3D-printing technologies available like laser sintering,[3] stereolithography or fused filament fabrication (FFF).[2] This work focused on the FFF technology, which describes the manufacturing of objects by applying layers of molten plastic through a heated extrusion nozzle. In comparison to the other mentioned 3D-printing methods, FFF printing is less expensive, and a wide range of different materials are available.[4,5]

Recently, the technological advancement of 3D-printing has led to increased interest of research for applications in the biotechnological context. The development of cultivation devices for mammalian cell cultures, where special geometries are necessary to induce cell differentiation and tissue formation is an example.[6–8] It is also applied for manufacturing of lab-on-a-chip systems,[9,10] cell immobilization devices or individualized labware.[11,12] The most recent applications even include 3D-printed foods or artificial organs for clinical studies.[13–16] Nevertheless, there are only a few studies available on 3D-printed bioreactors for bacterial cultivation. They either focus on microbioreactors or combine commercially available glass vessels with 3D-printed holders and components, which limits design freedom.[17,18] Nowadays, research on utilization of alternative substrates for sustainable bioproduction is increasing and 3D-printing can be used to develop new reactor concepts for tailor-made applications.[19,20] The major challenges for bacterial cultivation, however, is the high content of non-fermentable, potentially harmful substances that inhibit bacterial growth as reported by Arnold et al.[21] Using perfusion systems is a possible solution to utilize such substrates, since the continuous flow of the medium through the bioreactor prevents the accumulation of inhibitors.[6,21] Additionally, the retention with membranes reduces the risk to wash-out the bacterial cells, allowing dilute concentrations to be used at higher flow rates. 3D-printed perfusion bioreactors also offer benefits for optimization experiments or kinetic studies through parallelization. Because of the low manufacturing times and the affordable price, multiple bioreactors can easily be produced by 3D-printing and operated in parallel.[6,22] This enables simultaneous examination of different parameters, thus speeding up process development times.

With these applications in mind, a new concept for a 3D-printed perfusion bioreactor system is presented in this study. The bioreactor system with a volume of ~50 mL utilizes a hydrophilic flat sheet membrane for cell retention. It includes a circulation line for diffusive transfer of oxygen to the medium via a module that includes hydrophobic membranes for separation of gaseous and liquid phases. An electric heat exchanger combined with a PID-controller is used for temperature control. To evaluate the suitability of the system for bacterial cultivation, the mixing times and oxygen transfer coefficient were determined. Finally, a cultivation with *Corynebacterium glutamicum* ATCC 13032 on glucose was performed as proof-of-concept, which showed that the cultivation process can be maintained for at least 52 h up to a biomass concentration of 18.4 g L^{-1} without membrane blockage. In this way, this study provides a template of a 3D-printed perfusion bioreactor that facilitates the exploitation of alternative substrates without the need for expensive commercial equipment.

2 | MATERIALS AND METHODS

2.1 | Analytics and chemicals

If not stated otherwise, the chemicals used in this work were obtained from Carl Roth GmbH (Karlsruhe, Germany). Morpholino propanesulfonic acid (MOPS, order number 1081) as buffering agent was obtained from GERBU Biotechnik GmbH (Heidelberg, Germany). Enzymatic assay kits from R-biopharm AG (Darmstadt, Germany) were obtained for analysis of glucose (Cat No. 10716251035) and lactate (Cat. No. 11112821035).

2.2 | The 3D-printed perfusion bioreactor system and its operating conditions

The main flow through the system is generated by two syringe pumps (Cetoni neMESYS 290N, Cetoni GmbH, Corbussen, Germany) with 10 mL single-use syringes (Omnifix 10 mL with Luer Lock, B.Braun AG, Melsungen, Germany). A 1-to-10 valve module (Cetoni Qmix V Ex, Cetoni GmbH, Corbussen, Germany) allows switching between different feeding or sterilization solutions (Figure 1A). In front of the main entrance to the bioreactor a pressure probe and a 3-2-way valve were installed to monitor the pressure of the system followed by the main bioreactor module (Figure 1B) with ports for different probes, a sample port and the cell retention membrane as described in detail in Section 2.1.1. With the latter, the permeate leaves the bioreactor and is collected in a bottle. Stirring is used for mixing the reactor content (Figure 1C). Besides the main flow through the reactor, a six-channel peristaltic pump (Peristaltic Pump peRISYS-S, Cetoni GmbH, Corbussen, Germany) in combination with two 2-stopper flexible tubing (2.7 mm iD) is used to generate a circulation flow. The circulation flow is used for oxygen supply via membrane diffusion by an oxygen transfer module (Figure 1D) as well as for temperature control via a heat exchanger module (Figure 1E). Polytetrafluoroethylene (PTFE)-tubing with 1.6 mm inner diameter (iD) and 3.3 mm outer diameter (oD) in combination with corresponding ¼″−28 flat bottom fittings and ferrules were used to connect most modules of the system. To connect the PTFE-tubing to flexible tubing female Luer to ¼″−28 male adapters were used. All pumps, valves and pressure probes were controlled and monitored via the software Qmix elements (Cetoni GmbH, Korbussen, Germany). The corresponding 3D-models are provided in the supplementary information as .stl-files. A flow diagram and render pictures of the different modules are shown in Figure 1.

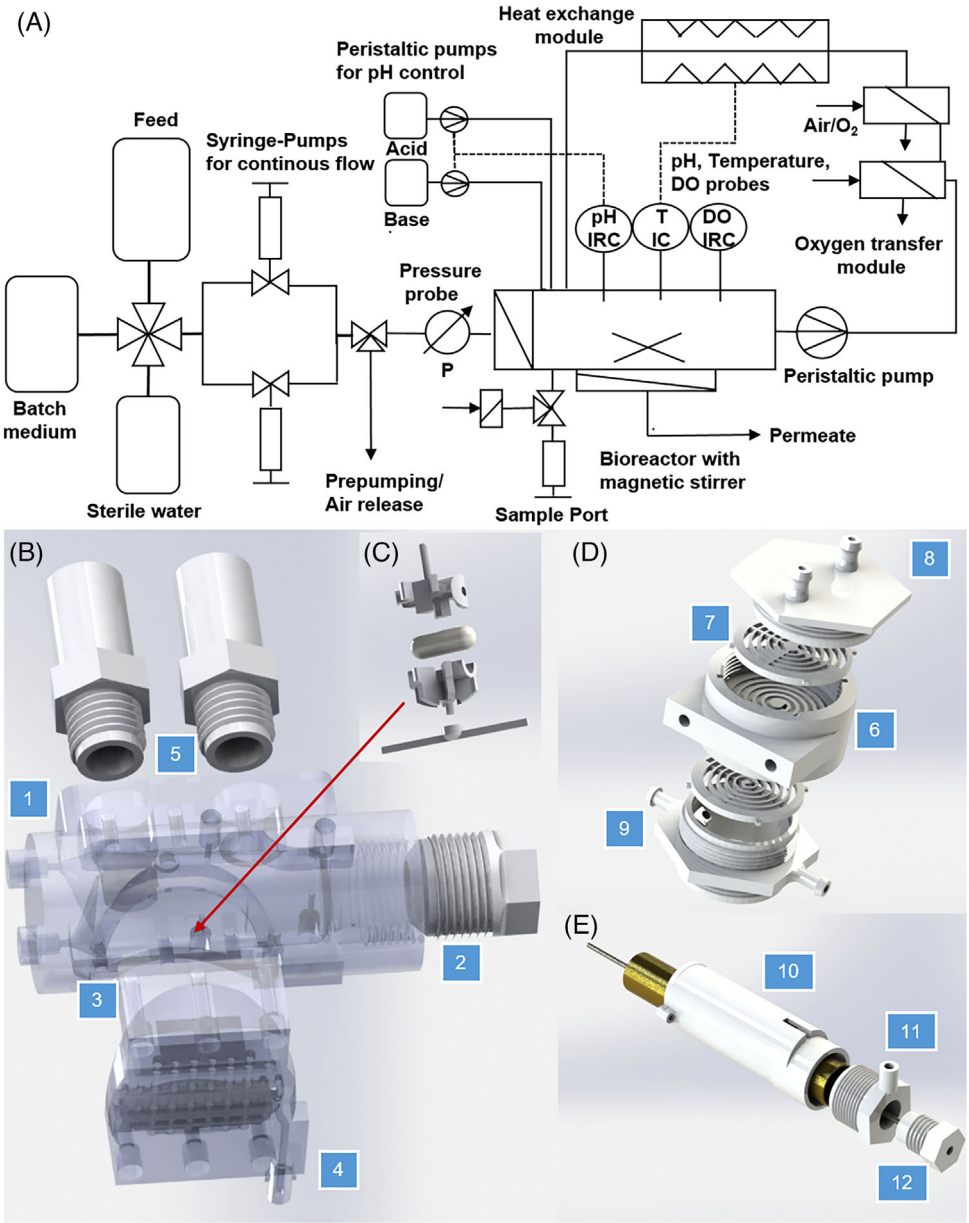

FIGURE 1 Layout and render pictures of the perfusion bioreactor system. (A) Flow chart of the bioreactor system. (B) Render picture of the bioreactor main body (1), the cap (2), cell retention membrane support (3 + 4) and probe connectors (5); (C) render picture of the 3D-printed stirrer frame; (D) render picture of half of the oxygen transfer module with connectors for gas tubing (8), a stabilizer (7), the liquid compartment, that has spiral flow channels on both sides which are covered by circular membranes (6), and a middle compartment with connectors for gas tubing (9). (E) Render of half of the heat exchange module, consisting of an encasing (10), a fitting with connections to fill the outer tube (11) and a cap for connection to the flow system of the culture broth (12). The brass tubing as well as the thin capillary in the middle are not 3D-printed.

2.2.1 | The main bioreactor module

The main component of the system is the bioreactor module shown in the exploded view in Figure 1B. The main bioreactor module has an oD of 41 mm and an iD of 24 mm. The lower half of the tube is horizontal, while the upper half has an outward slope with an angle of 4.4° (Figure S1, supporting information). At the reactor end, the tube splits and narrows into two 2-mm channels with two tap holes for ¼″−28 threading (Figure 1B1). At this point the circulation flow starts. The main inlet into the reactor (Figure 1B2) consists of a socket with M27 threading, in which a hydrophilic polyvinylidene difluoride (PVDF) membrane (Durapore, 0.22 μm pore size, 47 mm oD, Merck KGaA, Darmstadt, Germany), with 24 mm diameter, and a stabilizing grid are placed. The inlet is closed by the reactor cap with two tap holes for ¼″−28 threading. Starting from the inlet-membrane the inner tube of the bioreactor module has a height of 7.7 mm. Together with the iD of 2.4 mm this results in height-to-diameter ratio of 3.2 which is close to the typical ratio of ~3 for microbial bioreactors allowing best

mixing conditions.[23] Figure 1B3 shows the cavity, in which another hydrophilic PVDF membrane (diameter = 47 mm) with wide bearing area of 4 mm (effective membrane area of 12 cm^2) is placed for cell retention. The membrane is kept in place by the membrane support (Figure 1B4), which is fixed with six M3.5 screws and nuts. It was incorporated into the bioreactor's mantle to offer a high enough surface area to keep the pressure in the system caused by the transmembrane pressure low and to lower the risk of pressure spikes caused by membrane fouling as shown by Darcy's law: [24]

$$Q = \frac{k * A}{\eta} * \frac{dP}{L} \quad (1)$$

Q = flow rate in mL min^{-1}, k = permeability in Darcy, A = membrane area in cm^2, dP = pressure difference in bar, η = dynamic viscosity in kg m^{-1} s^{-1}, L = membrane/filter thickness in m.

The stirrer (Figure 1C) consists of a 3D-printed frame covering a magnetic stirrer bar (7 mm diameter, 20 mm long) and is placed above the membrane. In addition, Figure 1B5 marks two ports for pH or DO probes. The probe adapters are connected via M20 threading. Furthermore, on the sides of the reactor module five connections for ¼″−28 threading are placed. Another connection with a 3 mm channel is reserved for a Pt100 temperature probe. Three connections are used for the sample port and the pH-correction solutions (1 M HCl and 4 M NaOH), the last one as inlet for the circulation flow. For the pH-correction solutions, PTFE tubing with an oD of 1.6 mm was used, which could be pushed through the channels directly into the interior of the bioreactor to prevent contact between NaOH and the 3D-printing material. For the sample port, a Luer 3-2 way valve was added with a sterile filter at one end and a syringe on the other. In total, the reactor contains a volume of 39 mL. All probes, the bioreactor cap and the membrane support were sealed with o-ring gaskets.

2.2.2 | Liquid-gas membrane contactors for oxygen supply

For the reactor setup chosen in this work bubble aeration is not suitable, as the gas flow would have to be strictly controlled to prevent liquid expulsion from the reactor. Additionally, bubble aeration could cause foam formation, which leads to the same problem. Accordingly, oxygen supply via diffusion was chosen and an oxygen transfer module was constructed (Figure 1D), relying on hydrophobic PTFE membranes for separation of liquid and gaseous phases. One module consists of several compartments. The liquid compartment (Figure 1D6) with flow channels for the culture broth is equipped with two tap holes for ¼″−28 threading. The liquid follows spiral patterns on each side of the module, which are connected in the middle. The rectangular channels (1 mm deep and 2.3 mm wide) are covered by hydrophobic PTFE-membranes with an oD of 47 mm, a pore size of 0.22 μm and 85% porosity (Fluoropore membrane filter, Merck KGaA, Darmstadt, Germany) resulting in an effective membrane area of 8.7–9.0 cm^2. To seal the liquid compartment, a ring socket with 42 mm iD and 47.5 mm oD surrounds the spiral flow pattern, in which silicone gaskets with a strength of 2 mm are placed beneath the membrane. A plastic grid (Figure 1D7) that mimics the flow channels is placed on top of the membrane to prevent it from warping outwards. The module was set up in a way that allows increasing the membrane area by stacking multiple liquid and gas compartments (Figure 1D8 and D9) onto each other. Each liquid compartment contains a volume of ∼1 mL.

2.2.3 | Heating module for temperature control

The heat exchange module follows the principle of a double pipe heat exchanger. The outside pipe is a brass pipe (19 mm length, 25 mm oD, 1 mm strong) that is covered by an electric heating element (Thermo Tech Polyester heating foil, 30 W, 24 V). It is filled with water as heat transfer medium. The inner pipe is a stainless-steel pipe (21 mm length, 0.5 mm strength) with 2.1 mm iD, through which the culture broth is pumped. Brass was chosen as metal for the outer pipe, due to its superior thermal conductivity compared to stainless steel. The heating element as well as a PT100 temperature probe were connected to a PID controller (ITC-100VL PID Temperature Controller 12–24 V, Inkbird, China) for temperature control. The temperature probe was placed into the bioreactor to measure the temperature at the main reaction compartment. 3D-printed holders (Figure 1E10) and a 3D-printed encasing (Figure 1E11) were used to separate the tubes and isolate the heating element from external factors. The heat exchange module adds 0.8 mL to the total reactor volume.

2.3 | Design and fabrication of the 3D-printed components

All 3D-printed components were constructed using the computer-aided design (CAD) software Solidworks 2018 (Dassault Systèmes SolidWorks Corporation, Waltham, USA). The designed CAD-files were then exported to .stl files (see supporting information for a list and description of included models) that could be imported and converted by the slicing-application for 3D-printers Cura (Ultimaker BV, Utrecht, Netherlands). Cura is an open-source software that converts 3D-objects into layer-based files, which can be used by most 3D-printers for manufacturing real objects. In this study, the FFF 3D-printers Ultimaker 3 and Ultimaker 3 extended (Ultimaker BV, Utrecht, Netherlands) outfitted with AA 0.4 mm brass nozzles were used. The Ultimaker 3 is equipped with a dual extrusion print head allowing the use of two different filament types at the same time. Additionally, the printing chambers of both printers were encased. This allowed higher temperatures on the inside of the printer and prevented disturbances from the outside, which is necessary for printing with most technical filaments. The 3D-printing filaments acrylonitrile butadiene styrene (ABS), CPE+, CPE from Ultimaker and nGen flex from ColorFabb (ColorFabb B.V., Belfeld, Netherlands) were used in this study. For

the Ultimaker materials, printing profiles were available in Cura, which were used as templates with some modifications. For nGen flex, the profile of CPE+ was used as template. The settings used for printing the different materials are given as part of the supporting information (Table S1).

Only threading with a size of M20 or higher could be printed when the tap hole had a vertical orientation. For all other threading-types special cutting tools (taps) were used. Since 3D-printing using the FFF principle often produces rough and porous surfaces, but clean surfaces are needed for sealing and waterproof prints, two methods were applied for smoothing. The first method is only applicable for ABS-prints, for which acetone vapor was used.[25] In detail, the objects to be treated were placed into a 1 L glass beaker filled with 30–50 mL of acetone, which was then heated to a temperature of 80°C for 25 min to generate the vapor. A glass inlet was used to prevent the objects from touching the liquid acetone. The top of the beaker was closed with aluminum foil. The second method was material independent and contained treatment of sealing surfaces with a two-component epoxy resin (XTC-3D, Smooth-On, Inc, Macungie, Pennsylvania).

2.4 | Determination of mixing time

Typically, the t_{95} value is determined to characterize the mixing efficiency (time to reach 95% of complete homogenization). In this work, a decolorization method based on iodometry was used.[26] Therefore, a 0.05 g L^{-1} starch solution colored by addition of 12 mL L^{-1} 1% iodine/potassium iodide solution was filled into the bioreactor system. After a stable circulation flow was achieved, 4 mL L^{-1} 0.1 M sodium thiosulfate heptahydrate solution was added via syringe for decolorization. The time until complete decolorization of the starch solution is then defined as t_{95}. A camera was used to document the mixing experiments.

2.5 | Determination of oxygen transfer rates

The dynamic gassing-out method according to Van't Riet was used for determination of oxygen transfer rates.[27] First, oxygen was removed from the solution by nitrogen aeration. Subsequently, aeration was switched to pure oxygen and the dissolved oxygen (DO) was measured with a probe. The oxygen transfer rate was calculated from the slope of the DO curve according to equation 1:

$$\dot{M}_{O2} = V_R * \frac{c_{O2}(t) - c_{O2}(t_0)}{t - t_0} \quad (2)$$

$\dot{M}_{O2}$ = oxygen mass transfer in mg h^{-1}, $c_{O2}(t)$ = oxygen concentration and $c_{O2,s}$ = oxygen solubility in mg L^{-1}, V_R = Reactor volume in L, t = time in h.

A 35 g L^{-1} NaCl-solution was used as substitute for typical media, since solubilities for this solution are available.[28]

2.6 | Cultivation conditions

2.6.1 | Bacterial strain and cultivation medium

The bacterial wildtype strain *C. glutamicum* ATCC 13032 was used for all cultivations performed in this study. The inoculum and media were prepared as described in an earlier publication, with the difference that glucose instead of acetate was used as the sole carbon source.[29] The medium composition $CGXII_F$ was used for shake flask cultivations and as batch medium for cultivations in the perfusion bioreactor with a pH value of 7.[29] For experiments with the perfusion bioreactor, $CGXII_{Perfusion}$ was used as feed medium during the continuous phase:

5 g L^{-1} glucose, 0.5 g L^{-1} KH_2PO_4, 0.5 g L^{-1} K_2HPO_4, 0.13 g L^{-1} $MgSO_4 \times 7\,H_2O$, 0.01 g L^{-1} $CaCl_2 \times 2\,H_2O$, 21 g L^{-1} MOPS, 0.2 mg L^{-1} D-biotin and 0.5 mL L^{-1} trace element solution (TES).

In comparison to the medium composition $CGXII_F$ most concentrations (besides $CaCl_2$ and D-biotin) were halved to prevent precipitation.

2.6.2 | Determining the effects of 3D-printed filaments on cell growth

Shake flask cultivations were performed to determine potential effects on the cell growth of *C. glutamicum* caused by the presence of 3D-printing materials. Therefore, the different 3D-printing filaments used during this study, ABS, CPE+, nGen flex, were cut to 1–2 cm pieces, sterilized by autoclaving and added to 500 mL shake flasks containing 50 mL $CGXII_F$ medium. For each filament, 10 g of pieces were added to one shake flask. Additionally, the experiment was also performed with pieces of CPE+ covered in epoxy resin. As control, a cultivation without filaments was performed. All cultures were inoculated to a starting optical density (OD_{600nm}) of 1.

2.6.3 | Cultivation in the perfusion bioreactor

For bioreactor cultivations, the 3D-printed perfusion bioreactor system described before was used. For measurement of DO and for pH-control, the reactor was equipped with a DO (VisiFerm DO 225; Hamilton Hamilton Company, Reno, USA) and a pH probe (EasyFerm Bio K8224; Hamilton Company, Reno, USA), which were connected to a data station of a 2 L bioreactor (Labfors 4, Infors AG, Bottmingen, Switzerland). The pumps and the pH controller of the Labfors were used for addition of pH-control solutions. At the beginning of the cultivation, air was used for oxygen transfer. When the DO concentration became limiting, pure oxygen was used instead. The cultivation temperature was controlled at 30°C by using a PID controller connected to a temperature probe and to the heating module described before. To start a cultivation, the culture broth was inoculated to a starting OD_{600nm} of 1 using the sample port. The pH control was set to a value of 7.0 with the pH control solutions 1 M HCl and 4 M NaOH.

Sterilisation of the main bioreactor compartment and the fluidic control system was performed with 70% ethanol using the peristaltic pump of the circulation line. After filling, the ethanol solution was connected to the syringe pumps and pumped through the perfusion system at a flow rate of 1 mL min^{-1}. At the same time, the peristaltic pump was set to 30 mL min^{-1} for distributing the ethanol through the system. After 1 h of sterilization, the bioreactor module was disconnected from the pumps, manually rinsed, and filled again with sterile water beneath the laminar flow. After reconnecting, an additional volume of 400 mL sterile water was pumped through the system to rinse off all remaining traces of ethanol at a flow rate of 0.5 mL min^{-1}. The oxygen transfer module was sterilized separately from the remaining bioreactor system. For sterilization of the oxygen transfer module, 1 M NaOH was used and incubated for 1 h at room temperature beneath the laminar flow, followed by careful rinsing with 50 mL of sterile water.

After both modules were sterilized, they were reconnected beneath the laminar flow cabinet and the pH and DO probes were installed. Finally, the whole system was flushed and filled with medium at a flow rate of 3 mL min^{-1} for 1 h using the syringe pumps.

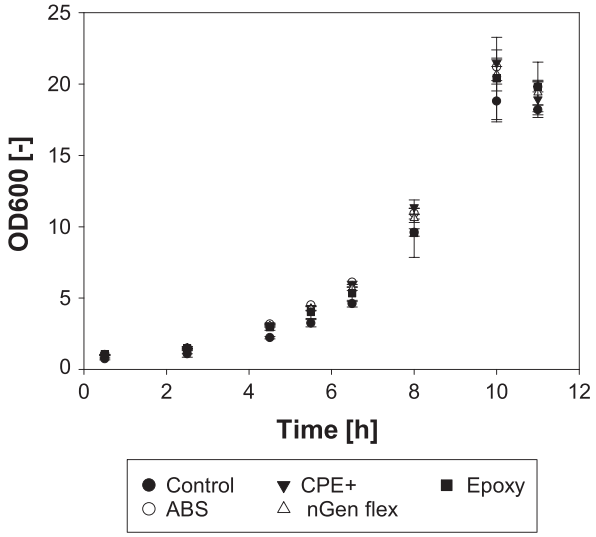

FIGURE 2 Time course of optical densities for *C. glutamicum* ATCC 13032 grown in the presence of 3D-printing filament pieces. 10 g of filament pieces were added to 50 mL of CGXIIF-medium using 10 g L^{-1} glucose as carbon source.

2.7 | Sampling and offline analytics

During cultivations, samples were taken every 2 h. The OD_{600nm} was determined using a spectrophotometer (Biochrom WPA CO8000, Biochrom Ltd., Cambrigde, United Kingdom) to monitor the cell growth. The biomass concentration was determined with a OD_{600nm} correlation factor of 4.3, determined in a previous study.[29] A volume of 0.5 mL of cell-free supernatant was prepared by centrifugation of each sample for 10 min at 14,000 rpm and 4°C (5430 R, Eppendorf AG, Hamburg, Germany). The supernatants were stored at −20°C. Glucose and lactate concentrations were determined using a spectrometer (Genesys 150 UV/Vis, Thermo Fisher Scientific GmbH, Braunschweig, Germany) and enzymatic assays from R-biopharm AG (Darmstadt, Germany), according to the manufacturer's protocols.

2.8 | Data analysis

Data analysis was performed using Microsoft Office Excel (Microsoft Corporation, Redmont). Maximum specific growth rates μ_{max} [h^{-1}] were determined by linear regression of a semi-logarithmic plot of OD_{600nm} against time with at least four sample points and a R^2 higher than 0.99. Biomass yields $Y_{X,S}$ [$g_{biomass}/g_{glucose}$] were calculated by linear regression of the accumulated biomass (dm_x) and the mass of glucose consumed during the same time (dm_s). At least four sample points were included with a R^2 higher than 0.95. Linear regression was also used for determining oxygen transfer rates by plotting DO against time as described in Section 2.5. During the experiment DO was recorded every 5 s until saturation. R^2 was higher than 0.99 for all conditions tested. Standard deviations were calculated using the "STDEV" function of Microsoft Excel.

3 | RESULTS

3.1 | Selection of 3D-printing filaments

Different types of plastic filaments are available for 3D-printers following the FFF-principle. The filaments used in this work were chosen based on their chemical resistance and thermal stability according to the manufacturers' technical data sheets. Accordingly, the following materials were chosen for manufacturing the bioreactor: Ultimaker ABS (deformation temperature (T_D) of 87°C) and Ultimaker CPE+ (T_D of 100°C). Colorfabbs nGen flex was also considered as an additional material because it is autoclavable. But since printed objects were not waterproof, it was not used for the final bioreactor.

Instead, CPE+ was used as 3D-printing material for the bioreactor's main body and for smaller parts like Y- or T-connectors due to its superior mechanical stability, when compared to ABS. The main body was exposed to increased tension because of the high number of connections via threading. One drawback of CPE+ was its intolerance for NaOH, which was intended to be used as sterilization agent because heat sterilization was not applicable. Ethanol, as alternative, wets the hydrophobic PTFE membranes of the oxygen transfer modules, making them permeable for aqueous solutions. Accordingly, ABS was used for manufacturing the oxygen transfer module, as it proved to be tolerant for contact with 1 M NaOH even for extended periods of time (over 24 h). The different modules were sterilized independently from each other according to Section 2.8 and reconnected aseptically.

To examine the impact of the 3D-printing materials on bacterial growth, shake flask cultivations with *C. glutamicum* ATCC 13032 were performed with pieces of the different filaments (CPE+, ABS, nGen flex or CPE+ covered with hardened epoxy resin, see Figure 2). Compared to the control all cultures with filaments showed a reduction of 10% in

μ_{max} (from 0.42 ± 0.01 1 h^{-1} to 0.36 ± 0.01 1 h^{-1}), while the maximum biomass concentration was unaffected (4.9 ± 0.4 g L^{-1}). Altogether, even though a small reduction in cell growth was determined, sufficient μ_{max} of 0.36 ± 0.01 1 h^{-1} was achieved.

3.2 | Evaluation of oxygen transfer

The construction of the oxygen transfer module was based on model equations for diffusive mass transfer of oxygen into a moving liquid based on Fick's law.[30] In this study, a hydrophobic, non-wettable PTFE membrane was used. A high solubility of oxygen in PTFE, a porosity of 85% and the low solubility of oxygen in water (8.3 mg L^{-1} at 25°C) led to the assumption that the mass-transfer-resistance on the liquid side is limiting for oxygen supply.[30–32] Accordingly, Equation (3) was used for calculating the mass transfer of oxygen into a flowing medium $\dot{M}_{O2}$, considering only the mass transfer coefficient on the liquid side β_L:

$$\dot{M}_{O2} = \beta_L * A * c_{O2,s} \tag{3}$$

β_L = liquid mass transfer coefficient in cm/s.

β_L can be calculated from the Sherwood number *Sh*, a dimensionless number describing the ratio of convective to diffusive mass transfer according to Equation (4):

$$Sh = \frac{d_h * \beta_L}{D} \tag{4}$$

Sh = dimensionless Sherwood number, d_h = characteristic diameter in m, *D* = diffusion coefficient in cm^2/s.

The analogy between heat and mass transfer was used for calculation of *Sh*, Thus, dimensionless Nusselt-numbers were replaced with Sherwood-numbers and Prandtl-numbers with Schmidt-numbers. As no equations for heat transfer with forced convection in non-circular channels were available, heat transfer in a narrow slit was used as an approximation.[33]

The Reynold's number *Re* and the characteristic diameter for a narrow slit d_h were calculated to determine the flow pattern of the medium in the channels according to Equations (5–7). The flow is considered laminar for $Re < 2300$ and turbulent for $Re > 10^5$. The flow pattern strongly influences substance transfer as it effects the thickness of boundary layers, the degree of radial mixing between flow layers as well as the distribution of flow speed.

$$d_h = 2 * s \tag{5}$$

$$Re = \frac{d_h * u}{\vartheta} \tag{6}$$

$$u = \frac{Q}{A_{cross}} = \frac{Q}{60 * s * b} \tag{7}$$

s = channel height in cm, *Re* = dimensionless Reynolds number, *u* = flow velocity in cm/s, ϑ = kinematic viscosity in cm^2/s, A_{cross} = channel cross area in cm^2, *b* = channel width in cm.

Restrictions caused by the 3D-printer and pumping equipment used in this work limited the range of flow rates and channel sizes to ranges where a laminar flow pattern is achieved. Thus, Equations (8–11) for the laminar flow through a narrow slit were used for calculating the mean *Sh*.

$$Sh = \left(Sh_1^3 + Sh_2^3\right)^{1/3} \tag{8}$$

$$Sh_1 = 4.861 \tag{9}$$

$$Sh_2 = 1.841 * \left(Re * Sc * \frac{d_h}{l}\right)^{1/3} \tag{10}$$

$$Sc = \vartheta / D \tag{11}$$

Sc = dimensionless Schmidt number, *l* = channel length in cm.

Equation (8) is valid in case that mass transfer only takes place from one side of the rift. This is true for the oxygen transfer module since oxygen can only be transferred from the membrane side but not from the channel bottom. Combining Equations (3–11) allows estimation of the oxygen mass transfer rate. Solubilities of oxygen can be found in literature.[34] Figure 3A shows a comparison between measured values of the oxygen permeability for the module as described in Section 2 and the values calculated with the equations above for different flow rates (10, 20, 30, 40, and 50 mL min^{-1}). For this experiment 3.5% NaCl-solution in water was chosen to mimic typical medium osmolarity. Two liquid compartments with an effective membrane area of 35.7 cm^2 were used. Pure oxygen was used for the gaseous phase and the temperature was controlled to 30°C, which is the typical cultivation temperature for *C. glutamicum*.[35] The experimentally determined mass flow coefficients correlated well with the coefficients calculated. This proves that the Sherwood correlation for thin channels was suited as a first approximation, when using rectangular channels. As expected, the highest mass transfer coefficient of 2.1 g h^{-1} m^{-2} bar^{-1} was determined with the highest flow rate of 50 mL min^{-1}. This resulted in a maximum oxygen transfer rate (OTR) of 161.6 mg L^{-1} h^{-1}. As expected for diffusion-based aeration, this is lower than the OTR achieved with typical stirred tank bioreactors, which can be as high as 9000 mg L^{-1} h^{-1} at maximum stirring and aeration rate (1200 rpm, 4 vvm).[36] Ways to increase the OTR are to increase the membrane area or the flow rate. With the pump used in this work, the maximum possible flow rate was 50 mL min^{-1}. Switching, for example, to a membrane pump would allow application of higher flow rates. For the test cultivations with *C. glutamicum* ATCC 13032, it was planned to use two of the oxygen transfer modules in series to increase the oxygen transfer rate to 236.0 mg L^{-1} h^{-1}.

3.3 | Determination of the perfusion bioreactor's mixing time

Table 1 shows a summary of important process parameters of the perfusion process, including mixing time t_{95}. Mixing time refers to the time

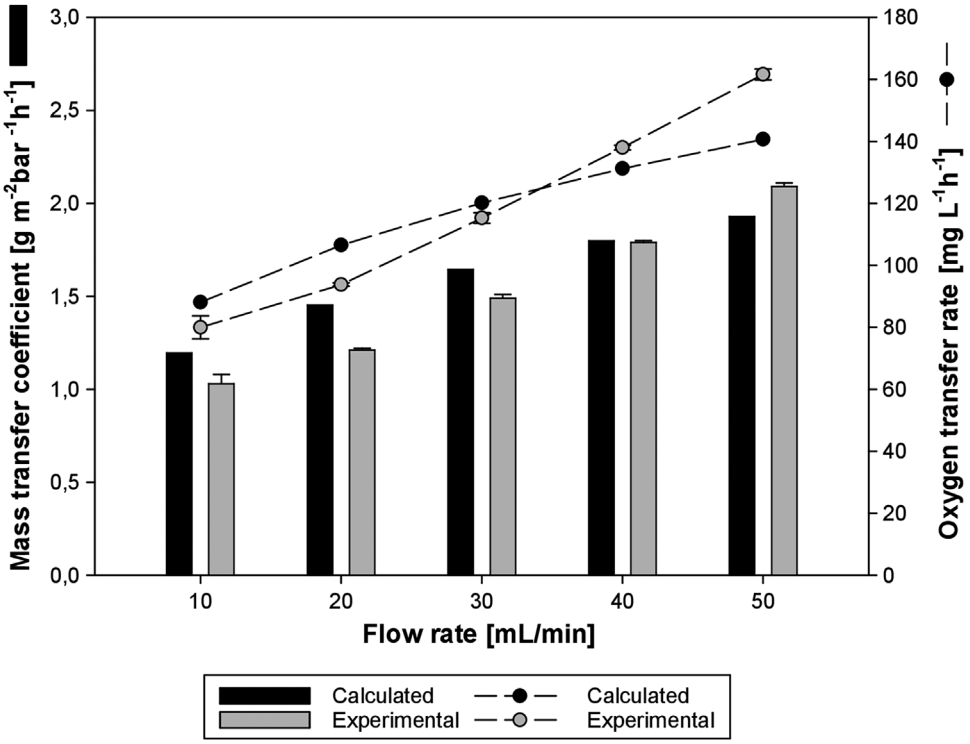

FIGURE 3 Summary of important process parameter. Comparison of oxygen transfer coefficients and rates experimentally obtained to mathematically estimated versions at different flow rates. Experimental conditions were 30°C, 35 g L^{-1} NaCl-solution as liquid medium and aeration with pure oxygen.

TABLE 1 Summary of important process parameters of the 3D-printed perfusion bioreactor.

Parameter	Unit	Value
Total volume[a]	mL	~50
Circulation flow rate	mL min^{-1}	30–50
Main flow rate	mL min^{-1}	0.25
t_{95}	s	63.3 ± 6.4
$t_{95,stirrer}$[b]	s	3.5 ± 0.6
Oxygen transfer rate[c]	mg/h	6.3–7.4
Oxygen mass transfer coefficient	g m^{-2} $bar^{-1}h^{-1}$	1.5–2.1
Membrane area, oxygen transfer[c]	cm^2	35.4
Membrane area, cell retention	cm^2	12.0
μ_{max}[d]	1 h^{-1}	0.34
Max. biomass concentration[d]	g L^{-1}	18.4

[a]Final volume depending on tubing length.
[b]With 300 rpm stirring speed.
[c]Determined with two liquid module parts.
[d]Determined with *C. glutamicum* ATCC 13032.

until 95% of total homogeneity is achieved. It was determined with the decolorization method described in Section 2.7. In a first configuration of the bioreactor system without stirrer, where mixing was achieved by circulation of the medium, a high mixing time of 63.3 ± 6.4 s was determined. This was due to the laminar flow conditions in the bioreactor at a circulation flow rate of 30 mL min^{-1}. To improve mixing, the magnetic stirrer and 3D-printed stirrer frame (see Figure 1C) were implemented into the bioreactor system, leading to a strongly reduced mixing time of 3.5 ± 0.6 s. The design of the stirrer resembles a plate impeller, a type of stirrer which is known to cause strong turbulences. It was placed directly above the membrane, as early perfusion experiments resulted in cells depositing on the membrane and forming a biofilm. The stirrer placement as well as the turbulences caused by it, prevented this effect. The unusual direction of the rotary axis (90°) was necessary to position the magnetic stirrer close enough to the stirring plate.

3.4 | Cultivation of *C. glutamicum* as proof-of-principle

To evaluate the suitability of the perfusion system for bacterial cultivation, a test cultivation was performed with the bacterial wildtype strain *C. glutamicum* ATCC 13032 on glucose as carbon source. In the beginning, a batch phase with 10 g L^{-1} of glucose was performed until a biomass concentration of 2.8 g L^{-1} was reached and 55% of the available glucose was consumed. At that point, a continuous feed with a flow rate of 0.25 mL min^{-1} was started, containing 5 g L^{-1} of glucose. Regarding oxygen transfer, pressurized air was initially used for diffusive oxygen transfer to prevent oxygen stress for the bacteria during the early growth phase. The circulation flow was set to 30 mL min^{-1} and the magnetic stirrer to 300 rpm. For pH control, 4 M NaOH and HCl

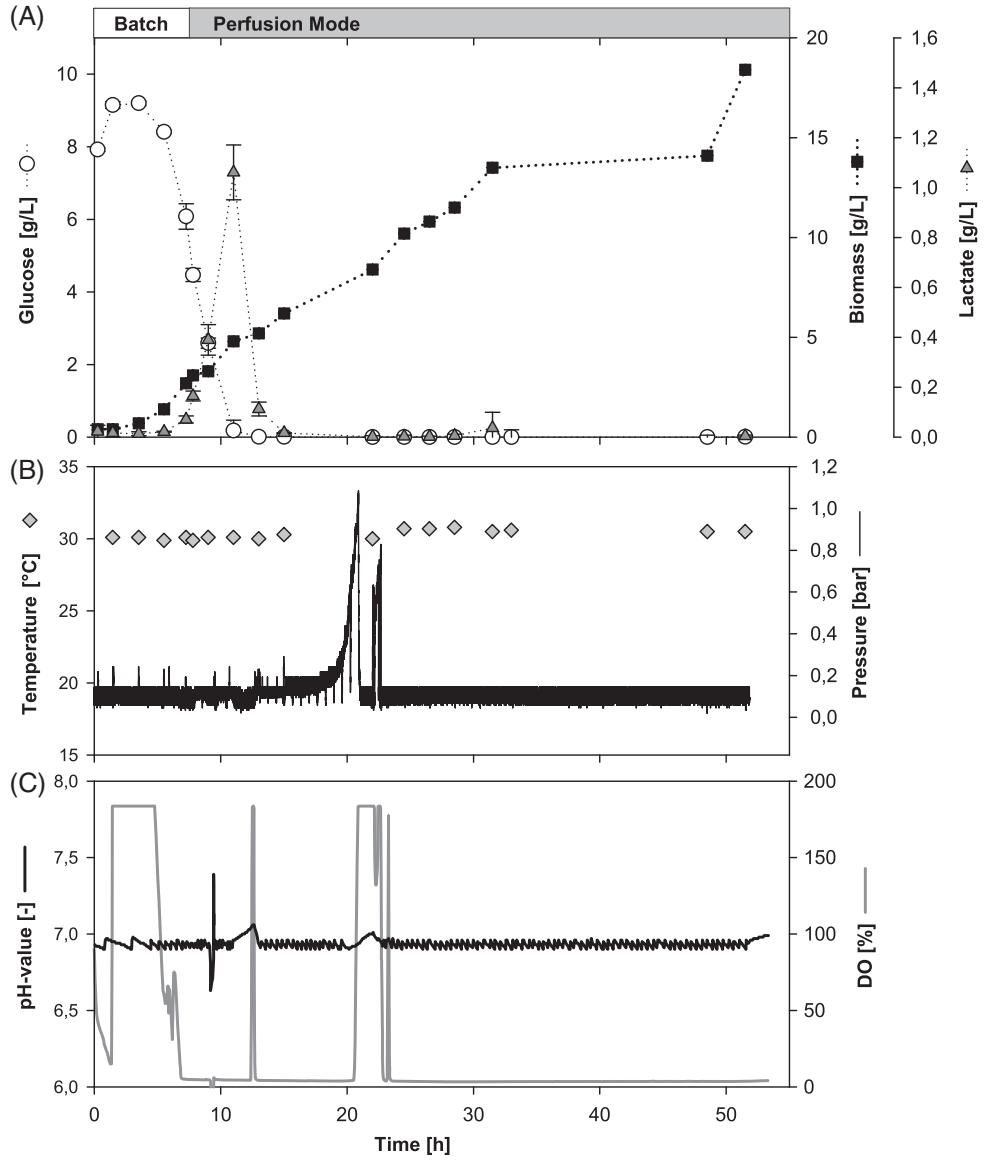

FIGURE 4 Cultivation data of a batch-perfusion hybrid cultivation of *C. glutamicum* ATCC 13032 performed in the 3D-printed perfusion bioreactor. The batch phase started with an initial glucose concentration of 10 g L^{-1}. At a biomass concentration of 3.1 g L^{-1}, the continuous feed containing 5 g L^{-1} glucose was started with a flow rate of 0.25 mL min^{-1}. Temperature was set to 30°C and pH to 7. (A) Time courses of glucose, biomass, and lactate concentration. Error bars show the standard deviation for a technical triplicate. (B) Time courses of temperature and pressure at the entrance to the bioreactor system. C) Time courses of the pH-value and DO.

were used to adjust the pH to 7.0. The time course of the cultivation data is provided in Figure 4.

While the bacteria were still adapting to the new medium composition, the air was sufficient for diffusive oxygen supply. When cell growth started after 1.4 h, the DO was quickly decreasing (Figure 4C). At a DO of 15.0%, pure oxygen was used for oxygen transfer, resulting in a DO-peak. After 4.8 h of cultivation, the DO started to decrease again and was depleted about 3.0 h later. During the time until oxygen depletion, the biomass concentration increased exponentially to 2.7 g L^{-1} (Figure 4A) with a μ_{max} of 0.34 1 h^{-1}. Overall, the oxygen supply was sufficient to allow an exponential growth until a biomass concentration of 3.3 g L^{-1} was reached after 9 h of cultivation. As quick consumption of the remaining glucose was expected after this time point, continuous feed was started with a flow rate of 0.25 mL min^{-1}. To allow strong mixing and turbulent flow conditions inside the main bioreactor module, the stirring rate was increased to 400 rpm. Growth of *C. glutamicum* continued with a gradual decrease to 0.05 1 h^{-1} until the process was stopped at a biomass concentration of 18.4 g L^{-1} after 51.5 h.

During the batch phase, growth of *C. glutamicum* resulted in a maximum biomass yield of 0.51 g g^{-1} glucose. After the feeding phase was started, the biomass yield decreased to 0.24 g g^{-1}, as oxygen depletion led to partially anaerobic conditions. This is shown by the drop in DO close to 0%. Nevertheless, the added glucose was completely consumed, as can be seen in Figure 4. Besides biomass, glucose was transformed to lactate, a side product which is typically produced

by *C. glutamicum* under anaerobic conditions.[37] In literature it was stated that *C. glutamicum* shows neglectable growth under anaerobic conditions and instead converted glucose to lactate, acetate and succinate.[38,39] While lactate was produced at the end of the batch phase during this cultivation, cell growth continued at a reduced rate of 0.05 1 h^{-1}. This suggests that cell growth was not completely under anaerobic conditions, as the oxygen transfer module still supplied the medium with oxygen, resulting in micro-aerobic conditions.

The pressure in the system is another important parameter especially for perfusion processes. During cultivations, it is a direct indicator for the degree of clogging of the cell retention membrane and thus of process stability. During the first 15 h after starting the continuous feed the pressure was stable at 0.2 bar. Subsequently, the pressure increased and peaked at 1 bar after 21 h. This peak was caused by clogging of the inlet membrane, potentially because of precipitated medium components and entrapped air bubbles. By removing the inlet membrane, the pressure could be reduced to 0.2 bar, proving that the main cell retention membrane was still free of blockage. Following this, the pressure remained constant until the end of the process after 44 h of feeding.

4 | DISCUSSION

In this work, a novel perfusion bioreactor system based on membrane diffusion for aeration and on hydrophilic flat sheet membranes for cell retention was developed using 3D-printing as manufacturing method. As described in Section 3.1 the 3D-printing materials CPE+ and ABS were selected for manufacturing different parts of the bioreactor, due to their respective mechanical stability and chemical resistances. The 10% reduction in specific growth rate μ_{max} observed in shake flask cultivations of *C. glutamicum* ATCC 13032 in presence of the different materials, was either caused by volatile additives of the plastic filaments,[40,41] or by the presence of solids and potentially hydrophobic surfaces, which is likely as all materials tested showed the same effect. Still, an observed μ_{max} of 0.36 1 h^{-1} allows for acquisition of data in a meaningful range, and the materials thus considered suitable for manufacturing the reactor.

Following the material selection, the oxygen transfer rate was evaluated, and the bioreactor's mixing time determined. For construction of the oxygen transfer module a combination of model equations for diffusive mass transfer into a moving liquid based on Fick's law and Sherwood correlations for thin channels were used. In an experiment the actual oxygen transfer rates at flow rates from 10 to 50 mL min^{-1} were determined and compared to the expected transfer rates, based on the model equations. Experimentally determined oxygen transfer rates of 80.0–161.6 mg L^{-1} h^{-1} aligned well with calculated values, showing that the model equations offer an accurate representation (Figure 3).

Regarding the mixing time, without a stirrer the mixing time t_{95} was 67 s and thus not efficient for providing a homogenous medium. To improve mixing, a magnetic stirrer encased in a 3D-printed frame was added, which reduced the mixing time to 3.5 ± 0.6 s at 300 rpm. This was comparable to commercial small scale bioreactors, which can achieve a mixing time between 5–20 s. [42] Besides a strong reduction of $t_{95,}$ the addition of the magnetic stirrer also reduced cell sedimentation and membrane fouling, as the stirrer was placed directly above the membrane. Consequently, this contributes to the ability to sustain longer process times.

The final step of the perfusion bioreactor's evaluation was a batch/perfusion hybrid cultivation of *C. glutamicum* ATCC 13032. During the batch phase, the specific growth rate μ_{max} of 0.34 1 h^{-1} was comparable to shake flask cultivations with the same medium composition in presence of 3D-printing materials (Section 3.1). Although oxygen became limiting after 7.3 h, growth continued at a reduced rate and a final biomass concentration of 18.4 g L^{-1} could be achieved after 51 h of cultivation. Furthermore, there was no clogging of the main cell retention membrane, while the pressure in the system remained constant at 0.2 bar for at least 44 h of feeding, indicating no or only limited clogging of the membrane system.

While bacterial cell growth continued even after oxygen depletion, depending on the intended application, it might be required to improve the oxygen transfer rate. This can be done by increasing the membrane area available for oxygen diffusion either by increasing the number of oxygen transfer modules or by upscaling the module and membrane size. In this respect, upscaling the module size and the size of the membrane circles used seems to be more efficient, as the increase in volume would be lower than for the other approach. Another option would be to switch to hollow fiber membranes. It should be considered however, that the use of hollow fibers would likely be more cost intensive.

In summary, a novel 3D-printed perfusion bioreactor system was presented, and its functionality demonstrated. Using a magnetic stirrer with a 3D-printed frame, homogenous medium conditions could be guaranteed in the main bioreactor, as shown by the mixing time of only 3.6 s. While a mass transfer coefficient for oxygen of 2.1 g h^{-1} m^{-2} bar^{-1} at a circulation flow rate of 50 mL min^{-1} was not enough to offer aerobic conditions above a biomass concentration of 2.7 g L^{-1}, it was still sufficient to support cell growth up to a biomass concentration of 18.4 g L^{-1} using *C. glutamicum* ATCC 13032 as model organism in a continuous cultivation experiment. Furthermore, pressure in the bioreactor remained constant at 0.2 bar even after 44 h of feeding in perfusion mode. This shows that only minor membrane fouling occurred, offering the potential for prolonged cultivation times. It should be considered however that perfusion processes come with innate disadvantages, which should be taken into account during the planning and design stage of a bioreactor system and process layout. These disadvantages include high amounts of perfused liquid and consequently diluted (extracellular) products, a potentially higher risk of contamination and a lack of data and comparable processes during the design stage of new processes. The described perfusion bioreactor system has broad application potential, from multi-component substrate-stream in a lignocellulose-based bioeconomy to in-situ product removal of potentially high-value products or even considerations of future applications for cultured meat by perfusion tissue cultures. As such, this work offers researchers a low-cost template for perfusion systems as well as a toolbox (all CAD files used or referred to in this

study are included as .stl files and described in the supporting information) with instructions for creating reference systems in different application scenarios or tailor-made bioreactor systems.

AUTHOR CONTRIBUTIONS

Manuel Merkel: Conceptualization, Methodology, Formal analysis, Validation, Investigation, Writing—Original Draft, Writing—Review & Editing, Visualization. Philipp Noll: Conceptualization, Methodology, Formal analysis, Investigation, Writing—Review & Editing. Lars Lilge: Conceptualization, Validation, Formal analysis, Writing—Review & Editing. Rudolf Hausmann: Conceptualization, Validation, Formal analysis, Writing—Review & Editing, Supervision, Funding acquisition. Marius Henkel: Conceptualization, Validation, Methodology, Formal analysis, Writing—Review & Editing, Supervision, Project administration, Funding acquisition.

ACKNOWLEDGMENTS

This study was partially funded by the Federal Ministry of Education and Research, Germany (BMBF, funding codes: 031B0673C). MM is a member of the "BBW ForWerts" graduate program funded by the Ministry of Science, Research and the Arts of Baden-Wuerttemberg (MWK).

Open access funding enabled and organized by Projekt DEAL.

CONFLICTS OF INTEREST STATEMENT

The authors declare no commercial or financial conflict of interest.

DATA AVAILABILITY STATEMENT

The data that supports the findings of this study are available in the supplementary material of this article.

ORCID

Marius Henkel https://orcid.org/0000-0002-5343-9661

REFERENCES

1. Schniederjans, D. G. (2017). Adoption of 3D-printing technologies in manufacturing: A survey analysis. *International Journal of Production Economics*, *183*, 287.
2. Melchels, F. P. W., Feijen, J., & Grijpma, D. W. (2010). A review on stereolithography and its applications in biomedical engineering. *Biomaterials*, *24*, 6121.
3. Kruth, J.-P., Levy, G., Klocke, F., & Childs, T. (2007). Consolidation phenomena in laser and powder-bed based layered manufacturing. *Cirp Annals*, *2*, 730.
4. Capel, A. J., Edmondson, S., Christie, S. D. R., Goodridge, R. D., Bibb, R. J., & Thurstans, M. (2013). Design and additive manufacture for flow chemistry. *Lab on A Chip*, *23*, 4583.
5. Gensler, M., Leikeim, A., Möllmann, M., Komma, M., Heid, S., Müller, C., Boccaccini, A. R., Salehi, S., Groeber-Becker, F., & Hansmann, J. (2020). 3D printing of bioreactors in tissue engineering: A generalised approach. *PLoS ONE*, *11*, e0242615.
6. Schmid, J., Schwarz, S., Meier-Staude, R., Sudhop, S., Clausen-Schaumann, H., Schieker, M., & Huber, R. (2018). A perfusion bioreactor system for cell seeding and oxygen-controlled cultivation of three-dimensional cell cultures. *Tissue Engineering Part C: Methods*, *10*, 585.
7. Balakrishnan, S., Suma, M. S., Raju, S. R., Bhargav, S. D. B., Arunima, S., Das, S., & Ananthasuresh, G. K. (2015). A scalable perfusion culture system with miniature peristaltic pumps for live-cell imaging assays with provision for microfabricated scaffolds. *BioRes. Open Access*, *1*, 343.
8. Smith, L. J., Li, P., Holland, M. R., & Ekser, B. (2018). FABRICA: A Bioreactor Platform for Printing, Perfusing, Observing, & Stimulating 3D Tissues. *Scientific Reports*, *1*, 7561.
9. Monaghan, T., Harding, M. J., Harris, R. A., Friel, R. J., & Christie, S. D. R. (2016). Customisable 3D printed microfluidics for integrated analysis and optimisation. *Lab on A Chip*, *17*, 3362.
10. Lockwood, S. Y., Meisel, J. E., Monsma, F. J., & Spence, D. M. (2016). A diffusion-based and dynamic 3D-printed device that enables parallel in vitro pharmacokinetic profiling of molecules. *Analytical Chemistry*, *3*, 1864.
11. Lücking, T. H., Sambale, F., Beutel, S., & Scheper, T. (2015). 3D-printed individual labware in biosciences by rapid prototyping: A proof of principle. *Engineering in Life Sciences*, *1*, 51.
12. Pantazis, A. K., Papadakis, G., Parasyris, K., Stavrinidis, A., & Gizeli, E. (2020). 3D-printed bioreactors for DNA amplification: Application to companion diagnostics. *Sensors & Actuators, B*, *319*, 128161.
13. Park, J., Wetzel, I., Dréau, D., & Cho, H. (2018). 3D Miniaturization of Human Organs for Drug Discovery. *Advanced Healthcare Materials*, *7*(2), https://doi.org/10.1002/adhm.201700551
14. Johnson, B. N., Lancaster, K. Z., Hogue, I. B., Meng, F., Kong, Y. L., Enquist, L. W., & McAlpine, M. C. (2016). 3D printed nervous system on a chip. *Lab on A Chip*, *8*, 1393.
15. Johansson, M., Nilsson, K., Knab, F., & Langton, M. (2022). Faba bean fractions for 3D printing of protein-, starch- and fibre-rich foods. *Processes*, *3*, 466.
16. Tejada-Ortigoza, V., & Cuan-Urquizo, E. (2022). Towards the development of 3D-printed food: A rheological and mechanical approach. *Foods*, *9*, 1191.
17. Guarino, A., Shannon, B., Marucci, L., Grierson, C., & Savery, N. (2019). A low-cost, open-source Turbidostat design for in-vivo control experiments in Synthetic Biology. *M. Di Bernardo*, *IFAC-PapersOnLine*, *26*, 244.
18. Hoffmann, S. A., Wohltat, C., Müller, K. M., & Arndt, K. M. (2017). A user-friendly, low-cost turbidostat with versatile growth rate estimation based on an extended Kalman filter. *PLoS ONE*, *7*, e0181923.
19. Zhang, B., Jiang, Y., Li, Z., Wang, F., & Wu, X.-Y. (2020). Recent progress on chemical production from non-food renewable feedstocks using Corynebacterium glutamicum. *Frontiers in Bioengineering and Biotechnology*, *8*, 606047.
20. Yaguchi, A., Spagnuolo, M., & Blenner, M. (2018). Engineering yeast for utilization of altiernative feedstocks. *Current Opinion in Biotechnology*, 122.
21. Arnold, S., Moss, K., Henkel, M., & Hausmann, R. (2017). Biotechnological perspectives of pyrolysis oil for a bio-based economy. *Trends in Biotechnology*, *10*, 925.
22. Kotz, F., Risch, P., Helmer, D., & Rapp, B. E. (2019). High-performance materials for 3D printing in chemical synthesis applications. *Advanced Materials*, *26*, e1805982.
23. Clapp, K. P., Castan, A., & Lindskog In, E. K. *Biopharmaceutical processing* (Eds: J, Günter, L, Eva, Ł, Karol, G, Parrish), Elsevier 2018, 457.
24. Whitaker, S. (1986). Flow in porous media I: A theoretical derivation of Darcy's law. *Transport in Porous Media*, *1*, 3.
25. Raveling, A. R., Theodossiou, S. K., & Schiele, N. R. (2018). A 3D printed mechanical bioreactor for investigating mechanobiology and soft tissue mechanics. *MethodsX*, 924.
26. Löffelholz, C., Husemann, U., Greller, G., Meusel, W., Kauling, J., Ay, P., Kraume, M., Eibl, R., & Eibl, D. (2013). Bioengineering parameters for single-use bioreactors: Overview and evaluation of suitable methods. *Chemie Ingenieur Technik*, *1-2*, 40.

27. Van't Riet, K. (1979). Review of measuring methods and results in nonviscous gas-liquid mass transfer in stirred vessels. *Industrial & Engineering Chemistry Process Design and Development*, *3*, 357.
28. Ramsing, N., & Gundersen, J., Seawater and Gases Tabulated physical parameters of interest to people working with microsensors in marine systems.
29. Kiefer, D., Merkel, M., Lilge, L., Hausmann, R., & Henkel, M. (2021). High cell density cultivation of *Corynebacterium glutamicum* on bio-based lignocellulosic acetate using pH-coupled online feeding control. *Bioresource Technology*, 125666.
30. Schneider, M., Reymond, F., Marison, I. W., & von Stockar, U. (1995). Bubble-free oxygenation by means of hydrophobic porous membranes. *Enzyme and Microbial Technology*, *9*, 839.
31. Ahmed, T., & Semmens, M. J. (1992). Use of sealed end hollow fibers for bubbleless membrane aeration: experimental studies. *Journal of Membrane Science*, *1–2*, 1.
32. Kreulen, H., Smolders, C. A., Versteeg, G. F., & van Swaaij, W. (1993). Microporous hollow fibre membrane modules as gas-liquid contactors. Part 1. Physical mass transfer processes. *Journal of Membrane Science*, *3*, 197.
33. Gnielinski, V., In: Stephan, P., Mewes, D., Kabelac, S., Kind, M., Schaber, K., Wetzel, T. (eds) *VDI-Wärmeatlas*, 1.
34. Ramsing, N., & Gundersen, J. (2011). Seawater and gases tabulated physical parameters of interest to people working with microsensors in marine systems. *Unisense*, https://unisense.com/wp-content/uploads/2021/10/Seawater-Gases-table.pdf (accessed 21 February 2020)
35. Eikmanns, B. J., Metzger, M., Reinscheid, D., Kircher, M., & Sahm, H. (1991). Amplification of three threonine biosynthesis genes in *Corynebacterium glutamicum* and its influence on carbon flux in different strains. *Applied Microbiology and Biotechnology*, *5*, 617.
36. Schaepe, S., Kuprijanov, A., Sieblist, C., Jenzsch, M., Simutis, R., & Lübbert, A. (2013). kLa of stirred tank bioreactors revisited. *Journal of Biotechnology*, *4*, 576.
37. Takeno, S., Ohnishi, J., Komatsu, T., Masaki, T., Sen, K., & Ikeda, M. (2007). Anaerobic growth and potential for amino acid production by nitrate respiration in *Corynebacterium glutamicum*. *Applied Microbiology and Biotechnology*, *5*, 1173.
38. Michel, A., Koch-Koerfges, A., Krumbach, K., Brocker, M., & Bott, M. (2015). Anaerobic growth of *Corynebacterium glutamicum* via mixed-acid fermentation. *Applied and Environmental Microbiology*, *21*, 7496.
39. Nishimura, T., Vertès, A. A., Shinoda, Y., Inui, M., & Yukawa, H. (2007). Anaerobic growth of *Corynebacterium glutamicum* using nitrate as a terminal electron acceptor. *Applied Microbiology and Biotechnology*, *4*, 889.
40. Thompson, M. S. (2022). Current status and future roles of additives in 3D printing—A perspective. *Vinyl Additive Technology*, *1*, 3.
41. Min, K., Li, Y., Wang, D., Chen, B., Ma, M., Hu, L., Liu, Q., & Jiang, G. (2021). 3D printing-induced fine particle and volatile organic compound emission: An emerging health risk. *Environmental Science and Technology Letters*, *8*, 616.
42. Nienow, A. W., Rielly, C. D., Brosnan, K., Bargh, N., Lee, K., Coopman, K., & Hewitt, C. J. (2013). The physical characterisation of a microscale parallel bioreactor platform with an industrial CHO cell line expressing an IgG4. *Biochemical Engineering Journal*, *76*, 25.

SUPPORTING INFORMATION

Additional supporting information can be found online in the Supporting Information section at the end of this article.

How to cite this article: Merkel, M., Noll, P., Lilge, L., Hausmann, R., & Henkel, M. (2023). Design and evaluation of a 3D-printed, lab-scale perfusion bioreactor for novel biotechnological applications. *Biotechnology Journal*, *18*, e2200554. https://doi.org/10.1002/biot.202200554